**PPPL-3238 - Preprint: February 1997, UC-420**

# The Role of the Neutral Beam Fueling Profile in the Performance of the Tokamak Fusion Test Reactor and other Tokamak Plasmas

H.K. Park, S.A. Sabbagh[a] , S. Batha, M. Bell, R.V. Budny, C. Bush[b] , Z. Chang, D. Johnson, D.K. Mansfield, D. McCune, K.M. McGuire, R. Nazikian, C. Skinner, R. Wieland, M. Yamada, and K.M. Young

*Princeton Plasma Physics Laboratory, Princeton University, Princeton, NJ 08543*

ABSTRACT

Scalings for the stored energy and neutron yield, determined from experimental data are applied to both deuterium-only and deuterium-tritium plasmas in different neutral beam heated operational domains in Tokamak Fusion Test Reactor. The domain of the data considered includes the Supershot, High poloidal beta, Low-mode, and limiter High-mode operational regimes, as well as discharges with a reversed magnetic shear configuration. The new important parameter in the present scaling is the peakedness of the heating beam fueling profile shape. Ion energy confinement and neutron production are relatively insensitive to other plasma parameters compared to the beam fueling peakedness parameter and the heating beam power when considering plasmas that are stable to magnetohydrodynamic modes. However, the stored energy of the electrons is independent of the beam fueling peakedness. The implication of the scalings based on this parameter is related to theoretical transport models such as radial electric field shear and Ion Temperature Gradient marginality models. Similar physics interpretation is provided for beam heated discharges on other major tokamaks.

PACS 52.55.Fa, 52.50.Gj, 52.25. Fi

a] Permanent address: Columbia University, New York, NewYork 10027

b] Permanent address: Oak Ridge National Laboratory, Tennessee 37830

## DISCLAIMER

## DISCLAIMER

Portions of this document may be illegible in electronic image products. Images are produced from the best available original document.

## I. Introduction

One of the goals of understanding plasma energy confinement is to provide guidance for the construction of future devices which will reach ignition of the fusion fuel. One approach toward fulfilling this goal in magnetic fusion research has been the statistical analysis of tokamak energy confinement, using tokamak plasma parameters as predictor variables. These studies normally produce formula, or "scaling laws" for tokamak energy confinement based on data gathered from several tokamak experiments worldwide.

Among the many scaling studies of tokamak energy confinement, the ITER-89P L-mode scaling [1] is well known and has been applied to most tokamaks around the world. While a high correlation with the chosen data has been achieved over the entire domain considered, significant improvements (and also degradations) of energy confinement, $\tau_E$ , have been produced in most tokamaks as compared to the International Thermonuclear Experimental Reactor (ITER) [2] scaling prediction. For example, in Tokamak Fusion Test Reactor (TFTR) [2], a large variation of the stored energy [~ 0.5 to ~3.5 times that computed from the ITER-89P L-mode scaling as shown in Fig. 1a] for beam heated discharges has been produced. This observation has motivated the consideration of new independent variables to better describe energy confinement and fusion power in TFTR. In particular, by introducing an independent variable related to the neutral beam fueling profile peakedness, a scaling with a smaller number of parameters and significantly reduced dispersion has been produced as shown in Fig. 1b.

It is demonstrated that the new scalings of energy confinement and neutron production can be applied to all beam heated deuterium (D) discharges in TFTR such as L-mode discharges (whose confinement times fit the empirical Low-mode (L-mode) scalings [3, 4]), the Supershot [5], High poloidal beta plasmas [6], discharges with a reversed shear (RS) magnetic configuration [7], limiter High-mode (H-mode) plasmas [8], and Supershots enhanced by Lithium (Li) pellet conditioning [9, 10]. These scalings were also applied to deuterium-tritium (DT) discharges. From the neutron scaling, one can estimate a scale factor between D and DT neutron yields. We find that the stored energy and neutron yield of TFTR neutral beam heated discharges are closely associated with the core fueling of the heating beams. We also find that the empirical relation between plasma ion energy content and the beam fueling parameter, $H_{ne}$, has a much different form than the relationship between electron energy content and the beam fueling parameter. The ion stored energy and fusion power production of the plasma are relatively insensitive to variations in plasma current, $I_p$, toroidal field, $B_T$, and safety factor, $q$, as compared to their dependence on $H_{ne}$. In contrast, the electron stored energy is relatively insensitive to $H_{ne}$, and has a greater dependence on plasma current. On the other hand, these plasma parameters are extremely important in determination of the stability boundary together with $H_{ne}$ [11]. The importance of $H_{ne}$ on the plasma performance has also been reported on other large neutral beam heated tokamaks [12, 13].

In section II, a brief summary of the modeled neutral-beam fueling profile shape factor [14] is provided. Here, the beam fueling profile shape factor is formulated as a function of plasma density and profile shape factor based on calculations. In section III, scalings with multiplication factors and exponents for the stored energy of each plasma species (ions and electrons) and the D neutron emission are provided. In section IV, further tests of the scalings for D discharges on new operating regimes such as Supershots at different major radii, enhanced Supershots with lithium conditioning, discharges with reversed shear magnetic configuration and DT discharges are discussed. Here, it is shown that the neutron production of discharges is not directly influenced by the toroidal field within the stability boundary where magnetohydrodynamic (MHD) activity is moderate [15]. In section V, we attempt to provide a connection of the scaling for ion stored energy to several key theoretical transport [16, 17, 18, 19] models. In section VI, the physics related to the beam fueling parameter in other major tokamaks based on published articles is reviewed.

## II. Heating beam fueling profile

The definition as well as the detailed calculation of the computed neutral-beam particle deposition profile peakedness for TFTR are provided in Refs. [14, 20]. Following these studies, $H_{ne}$ is defined as the ratio of the central beam fueling rate to the volume averaged beam fueling rate. This definition is similar to the density peakedness factor $F_{ne} = n_e(0) / \langle n_e \rangle$, where $n_e(0)$ is the central electron density and $\langle n_e \rangle$ is volume-averaged electron density. Note that $H_{ne}$ is similar in definition to $H(0)$ established in the earliest days of neutral beam research [21]. When the beam has single energy component, $H_{ne} = H(0)$. The attenuation of the injected neutral-beam is to first order proportional to the local electron density, so a peaked neutral-beam deposition profile can be achieved at high density only with a peaked density profile in TFTR. In order to parameterize the expression of $H_{ne}$ for a larger database subset, a regression has been performed for values of $H_{ne}$ calculated by the Transport (TRANSP) code [22] as a function of line-averaged electron density and the density peakedness factor. Among the functional combinations, the best description is given by

$$H_{ne} = 2.41 F_{ne}^{1.04} EXP(-0.24 \times 10^{-19} \bar{n}_e), \qquad [1]$$

and shown in Fig. 2, where $F_{ne}$ and $\bar{n}_e$ (in $m^{-3}$) are the measured peakedness and line-averaged density of electrons. The relationship in Eq. [1] shows that a peaked electron density profile shape is essential for peaked deposition of the neutral beam at high density. This expression (with the same coefficients) is applicable to TFTR discharges at different major radius. This subject is discussed in further detail in section V.

Using the measured $F_{ne}(t)$ and $n_e(t)$, it is instructive to examine the time dependence of $H_{ne}$ together with other plasma parameters for typical TFTR discharges. Fig. 3 shows the temporal evolution of $H_{ne}$ for L-mode and supershot discharges at the same beam power $(P_B \sim 22\ MW)$. In the supershot, the initial central beam fueling is significantly greater than that in the L-mode plasma due to differences in the pre-beam electron density. The initial high level of central beam fueling is maintained in the Supershot $(H_{ne} \sim 3.0)$ as $n_e$ is increased, until a "Carbon bloom" [23] (accompanied by a sudden rise of edge electron density) occurs at about 3.8 sec. The degradation of $W_{tot}$ and neutron emission ($S_n$) is well correlated with the reduction in $H_{ne}$ $(\sim 3.0\ to \sim 1.0)$. For the L-mode plasma, the low initial beam fueling $(H_{ne} \sim 1.0)$ falls rapidly to ~ 0.3 so that subsequent to neutral beam injection (NBI), there is almost an order of magnitude difference in $H_{ne}$ between the supershot and L-mode plasmas. It is striking, however, that the accumulated $W_e$ in each discharge is similar in magnitude. Therefore $W_i$ in the supershot discharge is significantly greater than that of the L-mode discharge. The D neutron emission in the L-mode discharge is an order of magnitude smaller than in the supershot discharge. The strong dependence of $W_i$ on $H_{ne}$, and the relatively weak dependence of $W_e$ on $H_{ne}$ suggests that the two species should be considered separately when developing a scaling for total plasma energy in TFTR.

## III. Scalings for the stored energy and fusion reactivity

The empirical scaling of plasma stored energy and fusion neutron yield are derived using a database of approximately 870 TFTR deuterium discharges, constrained to deuterium gas fueled discharges only. The data points are taken at the time of peak global stored energy. In order to eliminate other possible strong parametric dependencies, this data set is constrained to fixed plasma major and minor radii of $R = 2.45\ m$, and $a = 0.8\ m$, and toroidal magnetic field $B_T = 4.0\ T$ and $4.8\ T$. A wide range of beam power $(5\ MW < P_B < 32\ MW)$ and plasma current $(0.9\ MA < I_P < 2.0\ MA)$ are included. In all discharges, the beam power exceeds the Ohmic power by a factor of ~> 5 to reduce the influence of Ohmic heating on confinement. Deuterium beams with $(90\ keV < E_{inj} < 110\ keV)$ are injected tangentially into the torus and the data are restricted to nearly balanced injection, i.e., $|(P_{co} - P_{ctr}) / (P_{co} + P_{ctr})| < 0.4$, where the subscript co and ctr refer to injection in the same and opposite direction with respect to the plasma current, respectively. The effect of highly co- or counter-NBI on the derived scalings is examined in section IV.

The total stored energy $W_{tot}$ is determined from magnetic measurements, so that both the thermal and fast-beam ion energies are included. The electron stored energy is calculated using the measured electron density and temperature profile. The ion stored energy is defined as $W_i = W_{tot} - W_e$, where $W_e$ is the electron stored energy. Note that $W_i$ consists of both thermal and fast beam-ions. In principle, the stored energy of fast-beam ions should be studied separately from thermal ions. However, it is difficult and somewhat arbitrary to distinguish thermal ions from fast-beam ions when the ion temperature, as inferred from the measured carbon impurity temperature, approaches the incoming beam-ion energy. If the conventional analysis is applied to supershot plasmas [24], the fast-beam ion fraction in the supershot discharge is very close to that of an L-mode plasma.

The observed scatter in the ion stored energy data at various heating power can be significantly reduced by utilizing the parameters $H_{ne}$ and $I_p$ as shown in Refs. [11, 20]. Most importantly, the role of $H_{ne}$ is much more significant than that of $I_p$. Thus the stored ion energy can be described well by using only $P_B$ and $H_{ne}$ as shown in Fig. 4a with the scaling

$$W_i(J) = C_1 P_B^{1.3}(MW) H_{ne}^{0.8}, \qquad [2]$$

where $C_1$ is $2.04 \times 10^4$. The fact that the stored ion energy scaling is nearly linearly correlated with the central beam fueling ($P_B H_{ne}$) has important implications. For a fixed $H_{ne}$, the heating beam power dependence is quite different from the conventional L-mode scaling ($\propto P_B^{0.5}$) as shown in Fig. 4b.

The parametric dependence of the electron stored energy is significantly different from that of the ion stored energy. The result is given as

$$W_e(J) = C_2 P_B^{0.7}(MW) I_P^{0.4}(A), \qquad [3]$$

where $C_2$ is 310. While $H_{ne}$ is important in the determination of the ion stored energy, it is not important in the determination of the electron stored energy. It is interesting to find that the parametric dependence of stored energy of electrons is characteristically similar to L-mode scaling of the total plasma stored energy. Note that the fraction of electron stored energy rapidly decreases from 0.75 to 0.35 as the performance is improved. This may explain why the plasma current is not an important predictor variable in the Supershot regime as the L-mode scaling would indicate. The total stored energy of beam heated discharges can be defined simply as

$$W_{tot}^P = W_i + W_e. \qquad [4]$$

In TFTR, the neutron emission rate, $S_n$, from DD reactions has a positive correlation near unity with the ion stored energy ($S_n = CW_i^{1.6} \propto P_B^{2.1} H_{ne}^{1.3}$) as shown in Fig. 5. This result can be understood based on the basic reaction argument. The fusion cross-section (<σv>) is proportional to $\sim T_i^2$ for the range of ion temperatures *(10 keV ~ 20 keV)* on TFTR. Since the neutron yield is not entirely due to the thermonuclear reaction, the dependence is expected to be less than square. Note that in Supershots, the neutrons from the combination of beam-target and beam-beam reactions are comparable to the neutrons from thermonuclear reactions. Using the same set of independent parameters employed in the study of energy confinement, the scaling result for the fusion yield is

$$S_n^P = CP_B^{2.2}(MW)H_{ne}^{1.3} / V_p(m^3), \qquad [5]$$

where C is $2.71 \times 10^{14}$ and $V_p$ is plasma volume.

Furthermore, we can define the fusion power gain for DD discharges, $Q_{DD}$, for a fixed plasma volume as

$$Q_{DD} = S_n^P / P_B \propto CP_B^{1.2}(MW)H_{ne}^{1.3}. \qquad [6]$$

As shown in this equation, $Q_{DD}$ is nearly linearly proportional to the central beam fueling. Therefore, it is most efficient to improve $Q_{DD}$ by increasing $H_{ne}$ for a given heating beam power.

## V. Further Application of the Scalings on TFTR

In this section, the applicability of the scalings derived in section III at fixed major radii is examined for plasma with improved limiter conditioning and maximum $\tau_E$, various major radii, different degrees of co and counter directed NBI, altered current profile shapes, and deuterium-tritium fuel. It is found that the functional forms of the original scalings can be retained, and that the data can be quantitatively represented by small changes to the constant multiplicative factors in the scalings for $W^p_{tot}$ and $S^p_n$.

It is found that the stored energy is not strongly correlated with the major radius explicitly. This is illustrated in Fig. 6a, where the ratio $(W_{tot} / W^p_{tot})$ is shown as a function of heating beam power for discharges at three different major radii. This variation in major radius was produced in part in recent D and DT discharges with enhanced limiter conditioning $(R_0 = 2.52\ m,\ V_p = 37\ m^3)$ [9, 10]. This has produced enhanced Supershot discharges with $\tau_E$ up to ~1.5 times that of the highest energy confinement time of the data base studied. In addition to these high performance discharges, an L-mode study was also recently performed with both D and DT plasmas with beam heated discharges at an even larger major radius $(R_0 = 2.62\ m,\ V_p = 46\ m^3)$. This data set includes discharges with a reversed shear (RS) magnetic configuration [7].

Since the scalings of section III were derived from data constrained to having nearly balanced injection of the heating beam, it is informative to examine if the scalings are directly applicable to discharges with strongly co or counter heating beam sources. Fig. 6b shows that the measured stored energy is consistent with the scaling for both nearly co $(P_{co}/P_B > 0.8)$ and counter $(P_{co}/P_B < 0.2)$ heating beam sources. Fig. 6c illustrates that D discharges (Li enhanced Supershot discharges, Supershot, and L-mode) with varying major radii and varying beam injection balance, fit reasonably well with the scaling $W^p_{tot}$.

Plasmas with significant variations to the current profile shape have been investigated in regard to the present scaling study. The achieved stored energy of the beam heated discharges with highly peaked current profiles (high $\ell_i$ ) is compared with the scaling. The ratio $(W_{tot}/W^p_{tot})$ reaches up to ~1.2 as shown in Fig. 7. On the other hand, discharges (~150 shots) with reversed shear (RS) magnetic configuration fit well with 0.8 x $W^p_{tot}$ as shown in Fig. 7. When the neutron production was examined for discharges with the RS configuration, the result was $0.65$ x $S^p_n$ , which matches the prediction based on the self-consistent relationship between neutron production and stored energy discussed in the previous section. The central beam fueling is exceptionally good for some discharges with enhanced reversed shear (ERS) configuration but the stored energy and fusion reactivity are well below the level of Supershot discharges if the same logistics on confinement and fusion reactivity are applied. The result may provide insight for future studies examining the role of the current profile shape on plasma confinement.

The initial DT experiments [25, 26] on TFTR showed that the stored energy of DT discharges is about 25% higher than that of comparable D discharges. This fact has been attributed to an isotopic effect [24] due to the usage of tritium. When the scaling $W^p_{tot}$ of the stored energy derived from D discharges is applied to DT plasmas, it is found that the stored energy of DT discharges (both Supershots and L-mode discharges) fits to $1.25$ x $W^p_{tot}$ as shown in Fig. 8a. Note that the DT discharges in this figure have a fuel ratio (T/(D+T)) ranging from 30% to 70%. Considering that there are many differences between deuterium and tritium beam sources as discussed in section 2, it would be desirable to have a comparison study of Ohmic deuterium and tritium plasmas where the energy of the neutral of D and T are identical, in order to clarify whether or not this difference is due to an intrinsic isotopic effect in the plasma rather than due to the heating beam sources.

## VI. Relationship to theoretical transport models

There have been many different theoretical models proposed to explain variations in $\tau_E$ in tokamaks. At present, research emphasis has been placed on two groups of studies: localized enhanced core transport based on *ExB* shear [19], and non-local enhanced core transport based on ion temperature gradient (ITG) marginality [16].

Transport models based on radial electric field shear, inherited from the interpretation of the L-mode to H-mode transition at the plasma edge, may be explicitly related to the physics basis of the beam fueling peakedness. Experimentally, the beam fueling profile is clearly instrumental in controlling the pressure profile via the ion channel as shown in Eq. 2. The $\nabla p_i$ controlled by $H_{ne}$ may be the dominant source of the radial electric field in the transport theory when the toroidal plasma rotation is small. In fact, the theoretical models require a justification for the usage of a steep pressure gradient as a driving source. Since the central beam fueling is experimentally responsible for the determination of the ion stored energy, as we have learned in the previous section, it may provide the theoretical physics mechanism that can suppress the turbulence and hence improve the confinement. Even though this model is not constrained by particular wall recycling conditions, a high central plasma pressure can only be driven by high $H_{ne}$ in TFTR. A low edge density (as a result of good wall conditioning) is therefore needed indirectly.

The non-local nature of the core transport model based on ITG marginality is associated with the edge plasma condition. This model also has many common features with confinement scaling based on $H_{ne}$, even though this parameter is not explicitly used in the ITG model. High edge ion and electron temperatures are key elements to reaching enhanced confinement in this model. Similarly, high central beam fueling would result in

TFTR in low recycling conditions when the edge temperature is high and the edge density is low. This in turn results in a peaked density profile in NB heated plasmas. The peaked density profile therefore leads to increased confinement in both the model and scaling.

It is important to note that a peaked electron density profile alone is not a sufficient condition to improve the stored plasma energy in beam heated discharges in TFTR. Beam heated discharges with highly peaked density profiles at extremely high line-averaged density produced by solid D pellet did not exhibit improved confinement with respect to L-mode confinement time. This result is consistent with the corresponding exponential decrease of $H_{ne}$ [Eq. 1] at sufficiently high density. A recent significant improvement in energy confinement and neutron production created by intense wall conditioning using Li-pellet injection [9,10] prior to the injection of the beam, can be examined with similar logistics. In this case, the wall conditioning techniques reduce and in some cases maintain a low edge density, which in turn allows improved beam penetration and increased $H_{ne}$ .

## VI. The role of beam fueling profile in the performance of other tokamaks

In the previous sections, it has been demonstrated that the significant variation of the energy confinement in TFTR with respect to ITER-89P L-mode scaling (which has been used as a basis of the ITER design) can be reduced substantially when considering a scaling based on beam fueling peakedness. Similar effects of $H_{ne}$ on the performance of beam heated discharges have been reported on other tokamaks (Refs. [12,13]), suggesting that the effect might be universal. For instance, the fusion power gain for beam heated discharges in JET [2] is shown to be "$Q_{DD} \propto P_B$ *(central)* " [12] which can be qualitatively interpreted as the derived result for TFTR (Eq. 6).

Even though, the neutral beam heating sources used in most tokamaks are more or less similar to the beam sources employed in TFTR, there are significant differences in the beam fueling profile due to the beam line arrangement and operating plasma positions. In addition to the differences in the beam line orientation and the plasma cross-sectional shape, the time evolution of plasma density profiles can significantly influence the dependence of the performance on $H_{ne}$ as well.

Shaped and diverted plasmas differ from circular plasmas in several ways including profiles that are generally broader. Due to the relatively small contact point of the divertor strike point with the wall, there is a distinct advantage in the particle influx control. However, it is surprising to find that there are similarities in the performance improvement in a diverted plasma with respect to the beam fueling. If the performance of beam heated discharges is largely due to the variation of $H_{ne}$, the shaping factors such as elongation and triangularity in a shaped plasmas can relax the required line-average density and/or peakedness of density profile required to attain a given value of $H_{ne}$.

The NBI systems on the JET tokamak have two different beam energies (~140 keV and ~80 keV) and allow on-axis tangential injection. However, recent modifications implemented for a divertor study have resulted in an off-axis tangential heating system due to the imposed upward shift of the plasma position due to the divertor. In this configuration, neutron production was significantly reduced compared to previous results [27]. Off-axis beam deposition may not be entirely responsible for the observed degraded performance following the installation of the new divertor system but it provides a logical interpretation of the result [27].

Differences in the beam fueling profile might also help explain the result that the plasmas with an increased triangularity in DIII-D[2] yielded improved performance [28]. while similar experiments on JET did not improve performance [27] whereas similar experiments In JET, increased triangularity implies that the central beam fueling is further degraded due to up-shift of the plasma center. Recent experimental results have demonstrated that the triangularity was not strongly correlated with the performance of discharges on DIII-D [29]. Also elongation variation (from $\kappa = 1.68$ to $\kappa = 1.94$) experiments in DIII-D showed improved energy confinement together with increased $H_{ne}$ [30]. The DIII-D tokamak has a tangential injection system with a beam energy of approximately ~ 80 keV. Furthermore, the recent high fusion gain results [31] from DIII-D suggest that the peakedness of the beam fueling (90 % central beam fueling) may be responsible for the enhanced fusion reactivity. The "DIII-D H-mode edge" discharges with increased $H_{ne}$ (up to ~4.5) have produced significantly enhanced neutron rates compared to broader profile very high (VH) modes (a factor of ~3) with the same heating beam power. Note that the neutron yield of the former discharges is comparable to the level of TFTR plasma for similar heating beam power and $H_{ne}$.

The JT-60U [2] tokamak is equipped with a flexible but mainly off-axis heating system for full size plasma ($V_p = 100\ m^3$) operation with a beam energy of approximately ~90 keV. On JT-60U, the discharges with the best performance have been created in the high poloidal beta, $\beta_p$, regime obtained when a relatively small plasma ($V_p = 37\ m^3$) was formed toward the high field side of the vacuum vessel. This configuration allows central beam fueling in the JT-60U plasma [32]. Note that the beam deposition is always hollow for a full size plasma on JT-60U. Although a successful initial attempt was made to unify results [18] between TFTR Supershot and JT-60U high $\beta_p$ regimes based on beam fueling profile shape, lack of reliable density information in the JT-60U high $\beta_p$

regime and possible intrinsic differences between divertor and limiter plasmas requires that additional research be performed to make detailed quantitative comparisons of the scalings in these machines.

## VII. SUMMARY

Scalings of the ion and electron energy, and neutron yield have been derived for TFTR beam heated plasmas which include L-mode, limiter H-mode, Supershot, high $\beta_p$, and reversed shear confinement regimes in TFTR. An important feature of this scaling study as compared to similar L-mode scaling studies is the substantial reduction of the number of independent variables required to produce a good fit to the data. This is made possible by the inclusion of an independent variable that models the peakedness of the beam fueling deposition profile. The ion and electron components of the plasma are separately analyzed. The ion stored energy is sensitive to the central beam fueling. The electron stored energy is found to be insensitive to $H_{ne}$ and a dependence on plasma current is observed. Scalings with fixed multiplication factors and exponents for the stored energy and neutron yields were applied to both D and DT discharges at different major radii, with various wall conditions, with different current profile shape, and varying NBI balance. Beam fueling peakedness plays an important role in transport models that incorporate an ion pressure gradient term (such as the ExB shear model). The edge condition required for TFTR to increase $H_{ne}$ is consistent with the edge condition needed for improved confinement in the ITG marginality model. The importance of the beam fueling parameter is also evident in other major tokamak plasmas.

## ACKNOWLEDGMENT

This work was supported by U.S. DoE contract No. DE-ACO2-76-CH03073 and DE-FG02-89ER53297. We would also like to thank Drs. R. Hawryluk and D. Meade for the support of this work.

## Figure Captions

Figure 1. (a) Measured stored energy for TFTR beam-heated plasmas is compared with that of the ITER 89P L-mode scaling. The range spans from ~0.5 to ~3.5 times that of ITER 89P L-mode scaling. (b) Measured stored energy for TFTR beam-heated plasmas is compared with that of the new scaling. The dispersion is reduced significantly. Here, DT discharges and reverse sheared discharges are multiplied by 1.25 and 0.8, respectively.

Figure 2. The beam fueling parameter is formulated as a function of line average density and profile shape. $H^{TRANSP}$ is calculated beam fueling peakedness from TRANSP.

Figure 3. The temporal evolution of $H_{ne}$ based on Eq. 1 with other plasma parameters such as global stored energy $(W_{tot})$, stored energy of electrons $(W_e)$, and line average density for the same heating-beam power $(P_B \sim 22\ MW)$; Solid --- - "supershot" discharge at $I_P = 1.4\ MA$ and dotted --- - L-mode discharge at $I_P = 2.0\ MA$. Average $H_{ne}$ value of the supershot is an order of magnitude higher than that of L-mode for the first half second.

Figure 4. The influence of $H_{ne}$ on the ion stored energy is demonstrated for beam heated discharges. (a) The ion stored energy is nearly a linear function of the central beam fueling parameter ($P_B^{1.3}\ H_{ne}^{0.8}$ ). (b) The ion stored energy is not correlated with "L-mode scaling".

Figure 5. The measured DD fusion neutron emission $S_n$ has a tight correlation with $CW_i^{1.6}(\propto P_B^{2.1}H_{ne}^{1.3} \propto S_n^P)$. Deviation from a square dependence can be attributed to the importance of beam target and beam-beam reactions in addition to the thermonuclear reaction.

Figure 6. (a) The ratio ($W_{tot}/W_{tot}^p$) is depicted as a function of heating beam power for discharges at three different major radius. (b) The ratio ($W_{tot}/W_{tot}^p$) is shown as a function of beam power for discharges with nearly co ($P_{co}/P_B > 0.8$) [triangle] and counter ($P_{co}/P_B < 0.2$) [square] heating beam sources. (c) Comparison of the measured and modeled $W_{tot}$ for D discharges at various operating conditions (Li-enhanced Supershots, Supershots, L-mode).

Figure 7. The ratio ($W_{tot}/W_{tot}^p$) for discharges from high $\ell_i$ experiments (peaked current profile) is compared to the H-factor. Discharges with RS magnetic configuration (hollow current profile) obtained at $R_O = 2.62\ m$ are compared with $W_{tot}^p$. The best fit is 0.8 x $W_{tot}^p$.

Figure 8. The measured stored energy of DT discharges (Supershots and L-mode discharges) with a DT mixture ranging from 30 % to 70 % is compared with $1.25 \times W_{tot}^p$. Multiplier 1.25 is attributed to the isotopic effect from the usage of tritium.

## References

[1] P.N. Yushmanov, T. Takezuka, K.S. Riedel, O.J.W.F. Kardaun, J.G Cordey, S.M. Kaye, D.E. Post, Nuclear Fusion **30** (1990) 1999

[2] World Survey of Activities in Controlled Fusion Research [Nuclear Fusion special supplement 1991], (International Atomic Agency, Vienna, 1991)

[3] R.J. Goldston, Plasma Phys. **26** (1984) 87.

[4] P.H. Rebut, P.P. Lallia, M.L. Watkins, in Plasma Physics and Controlled Nuclear Fusion Research 1988 (Pro. 12th Int. Conf. Nice, 1988), Vol.2, IAEA, Vienna (1989) 191.

[5] J.D. Strachan, M. Bitter, A.T. Ramsey, M.C. Zarnstorff, V. Arunasalam, M.G. Bell, N.L. Bretz, R. Budny, C.E. Bush, S.L. Davis, H.F. Dylla, P.C. Efthimion, R.J. Fonck, E. Fredrickson, H.P. Furth, R.J. Goldston, L.R. Grisham, B. Grek, R.J. Hawryluk, W.W. Heidbrink, H. Hendel, K.W. Hill, H. Hsuan, K.P. Jaehnig, D.L. Jassby, F. Jobes, D.W. Johnson, L.C. Johnson, R. Kaita, J. Kamperschroer, J. Knize, T. Kozub, B. LeBlanc, F. Levinton, P.H. LaMarche, D.M. Manos, D.K. Mansfield, K. McGuire, D.H. McNeill, D.M. Meade, S.S. Medley, W. Morris, D. Mueller, E.B. Nieschmidt, D.K. Owens, H. Park, J. Schivell, G. Schilling, G.L. Schmidt, S.D. Scott, S. Sesnic, J.C. Sinnis, F.J. Stauffer, B.C. Stratton, G.D. Tait, G. Taylor, H.H. Towner, M. Ulrickson, S. vonGoeler, R. Wieland, M.D. Williams, K.L. Wong, S. Yoshikawa, K.M. Young, and S.J. Zweben, Phys. Rev. Lett. **58** (1987), 1004.

[6] S.A. Sabbagh, R.A. Gross, M.E. Mauel, G.A. Navratil, M.G. Bell, R. Bell, M. Bitter, N.L. Bretz, R.V. Budny, C.E. Bush, M.S. Chance, P.C. Efthimion, E.D Fredrickson, R. Hatcher, R.J. Hawryluk, S.P. Hirshman, A.C. Janos, S.C. Jardin, D.L. Jassby, J. Mnaikam, D.C. McCune, K.M. McGuire, SS. Medley, D. Mueller, Y. Nagayama, D.K. Owens, M. Okabayashi, H.K. Park, A.T. Ramsey, B.C. Stratton, G. Taylor, R.M. Wieland and M.C. Zarnstorff, Phys. Fluids B **3** (8), (1991), 2277.

[7] F. Levinton, M.C. Zarnstorff, S.H. Batha, M. Bell, R.E. Bell, R.V. Budny, C. Bush, Z. Chang, E. Fredrickson, A. Janos, J. Manikam, A. Ramsey, S.A. Sabbagh, G.L. Schmidt,

E.J. Synakowski, and G. Taylor, Phys. Rev. Lett. **75** (1995), 4417.

[8] C. E. Bush, R.J. Goldston, S.D. Scott, E.D. Fredrickson, K.M. McGuire, J. Schivell, G. Taylor, Cris W. Barnes, M.G. Bell, R.L Boivin, N. Bretz, R.V. Budny, A. Cavallo, P.C. Efthimion, B. Grek, R.J. Hawryluk, K.W. Hill, R.A. Hulse, A. Janos, D.W. Johnson, S. Kilpatrick, D.M. Manos, D.K. Mansfield, D.M. Meade, H. Park, A.T. Ramsey, B. Stratton, E.J. Synakowski, H.H. Towner, R.M. Wieland, M.C. Zarnstorff, and S. Zweben, Phys. Rev. Lett. **65** (1990) 424.

[9] D.K. Mansfield, J.D. Strachan, M.G. Bell, S.D. Scott, R. Budny, E.S. Marmar, J.A. Snipes, J.L. Terry, S. Batha, R.E. Bell, M. Bitter, C.E. Bush, Z. Chang, D.S. Darrow, D. Ernst, E. Fredrickson, B. Grek, H.W. Hermann, K.W. Hill, A. Janos, D.L. Jassby, F.C. Jobes, D.W. JOhnson, L.C. Johnson, F.W. Levinton, D.R. Mikkelson, D. Mueller, D.K. Owens, H. Park, A.T. Ramsey, A.L. Roquemore, C.H. Skinner, T. Stevenson, B.C. Stratton, E. Synakowski, G. Taylor, A. Von Halle, S. vonGoeler, K.L. Wong, and S.J. Zweben, Phys. of Plasmas **2** (1995), 4252.

[10] D.K. Mansfield, K.W. Hill, J.D. Strachan, M.G.,Bell, S.D. Scott, R. Budny, E.S. Marmar, J.A. Snipes, J.L. Terry, S. Batha, R.E. Bell, M. Bitter, C.E. Bitter, C.E. Bush, Z. Chang, D.S. Darrow, D. Ernest, E. Fredrickson, B. Grek, H.W. Hermann, A. Janos, D.L. Jassby, F.C. Fobes, D.W. Johnson, L.C. Johnson, F.M. Levinton, D.R., Mikkelson, D. Mueller, D.K. Owens, H. Park, A.T. Ramsey, AL. Roquemore, C.H. Skinner, T. Stevenson, B.C. Stratton, E. Synakowski, G. Taylor, A. von Halle, S. von Goeler, K.L. Wong, S.J. Zweben, and TFTR Group., Phys. of Plasmas **3** (1996), 1.

[11] Park, H.K., and Sabbagh, S.A., "Effect of the neutral-beam fuelling profile on fusion power, confinement, and stability in TFTR". Submitted in Nuclear Fusion 1996.

[12] Thompson, E., Stork, D., de Esch, H.P.L., and the JET Team, Phys. Fluids B 5 (7), (1993) 2468.

[13] H.K., Park, M.G. Bell, M. Yamada, K. McGuire, S. Sabbagh, R.V. Budny, R. Wieland, S. Ishida, T. Nishitani, Y. Kawano, Y.Y. Kamada, T. Fujita, M. Mori, Y. Koide, H. Shirai, M. Kikuchi, and the JT-60 Team, in Proceedings of the 15th International Conference on Plasma Physics and Controlled Nuclear Fusion Research, (Seville, Spain,

1994), (International Atomic Energy Agency, Vienna, Austria) Vol. **2** (1995) 3.

[14] Park, H.K., C.W. Barnes, R. Budny, D. McCune, G. Taylor, and M.C. Zarnstorff, Nucl. Fusion, **32** (1992) 1042.

[15] Z. Chang, E.D. Fredrickson, J.D. Callen, K.M McGuire, M.G. Bell, R.V. Budny, C.E. Bush, D.S. Darrow, A.C. Janos, E.J. Synakowski, G. Taylor, M.C. Zarnstorff, and S.J. Zweben, Nucl. Fusion **34** (1994) 1309.

[16] M. Kotschenreutor, W. Dorland, M.A. Beer, G.W. Hammett, Phys. Plasmas **2** (1995) 2381.

[17] M.A., Beer, G.W. Hammett, "Gyrofluid simulation of tubulence suppression in revered shear experiments on TFTR", in Phys. Plasmas (1996).

[18] J.F. Drake, Y.T. Lau, P.N. Guzdar, A.B. Hassam, S.V. Novakovski, G. Rogers, and A. Zeidler, Phys. Rev. Lett. **77** (1996) 494.

[19] S.I. Itoh, and K.J. Itoh, J. Phys. Soc. Jpn. **59** (1990) 3098.

[20] H.K. Park, M.G. Bell, W.M. Tang, G. Taylor, M.Yamada, Nucl. Fusion, 34 (1994) 1272

[21] J.A. Rome, J.D. Callen, J.F. Clarke, Nucl. Fusion **14** (1974) 141.

[22] R.V. Budny, Nucl. Fusion, **34** (1994), 1247.

[23] A.T. Ramsey, C.E. Bush, H.F. Dylla, D.K. Owens, C.S. Pitcher, M.A. Ulricson, Nuclear fusion **31**, (1991) 1811

[24] S.D. Scott, V. Aranasalam, C.W. Barnes, M.G. Bell, M. Bitter, R.L Boivin, N. Bretz, R.V. Budny, C. E. Bush, A. Cavallo, T.K. Chu, S.A. Cohen, P. Colstock, S.L. Davis, D.L. Dimock, P.C. Efthimion, A. B. Erhrardt, R.J. Fonck, E.D. Fredrickson, H.P. Furth, R.J. Goldston, G. Greene, B. Grek, L.R. Grisham, G. Hammet, R.J. Hawryluk, H.W. Hendel, K.W. Hill, E. Hinnov, D.J. Hoffman, J. Hosea, R.B. Howell, H. Hsuan, R.A.

Hulse, K.P. Jaenig, A. Janos, D. Jassby, D.W. Johnson, L.C. Johnson, R. Kaita, C.Kieras-Philips, S. Kilpatrick, M.C. McCarthy, D.C. McCune, K.M. McGuire, D.H. McNeil, P.H. Larmarche, B. Leblac, R. Little, D.M. Manos, D.K. Mansfield, E. Mazzucato, D.M. Meade, S.S. Medley, D.R. Mikkelson, R. Motley, D. Mueller, J.A. Murphy, Y. Nagayama, R. Nazikian, D.K. Owens, H. Park, A.T. Ramsey, M. Redi, A.L. Roquemore, P.H. Rutherford, G. Schilling, J. Schivell, G.L. Schmidt, J. Stevens, B.C. Stratton, W. Stodiek, E.J. Synakowski, W.W. Tang, G. Taylor, J.R. Timberlake, H.H. Towner, M. Ulrickson, S. von Goeler, R.M. Wieland, M. Williams, J.R. Wilson, K.-L. Wong, S. Yoshikawa, K.M. Young, M.C. Zarnstorff, and S. Zweben,et al., Phys. Fluids **B 2** (1990) 1300.

[25] J.D. Strachan, H. Adler, P. Alling, C.Ancher, H.Anderson, J.L.Anderson, J.W.Anderson, V.Arunasalam, G.Ascione, D.Ashcroft, C.W.Barnes, G.Barnes, S.Batha, M.G.Bell, R.Bell, M.Bitter, W.Blanchard, N.L.Bretz, C.Brunkhorst, R.Budny, T.Burgess, H.Bush, C.E.Bush, R.Camp, M.Caorlin, H.Carnevale, S.Cauffman, Z.Chang, C.Z.Cheng, J.Chrzanowski, J.Collins, G.Coward, M.Cropper, D.S.Darrow, R.Daugert, J.DeLooper, H.Duong, L.Dudek, R.Durst, P.C.Efthimion, D.Ernst, J.Faunce, R.Fisher, R.J.Fonck, E.Fredd, E.Fredrickson, N.Fromm, G.Y.Fu, H.P.Furth, V.Garzotto, C.Gentile, G.Gettelfinger, J.Gilbert, J.Gioia, T.Golian, N.Gorelenkov, B.Grek, L.R.Grisham, G.Hammett, G.R.Hanson, R.Hawryluk, W.Heidbrink, H.W.Herrmann, K.W.Hill, H.Hsuan, A.Janos, D.L.Jassby, F.C.Jobes, D.W.Johnson, J.Kamperschroer, J.Kesner, H.Kugel, S.Kwon, G.Labik, N.T.Lam, P.H.LaMarche, E.Lawson, B.LeBlanc, M.Leonard, J.Levine, F.M.Levinton, D.Loesser, D.Long, M.J.Loughlin, J.Machuzak, D.K.Mansfield, M.Marchlik, E.S.Marmar, R.Marsala, A.Martin, G.Martin, V. Mastrocola, E.Mazzucato, R.Majeski, M.Mauel, M.P.McCarthy, B.McCormack, D.C.McCune, K.M.McGuire, D.M.Meade, S.S.Medley, D.R.Mikkelsen, S.L.Milora, D.Mueller, M.Murakami, J.A.Murphy, A.Nagy, G.A.Navratil, R.Nazikian, R.Newman, T.Nishitani, M.Norris, T.O'Conner, M.Oldaker, J.Ongena, M.Osakabe, D.K.Owens, H.Park, W.Park, S.F.Paul, Yu.I.Pavlov, G.Pearson, F.Perkins, E.Perry, R.Persing, M.Petrov, C.Kieras-Phillips, S.Pitcher, S.Popovichev, R.Pysher, A.L.Qualls, S.Raftopoulos, R.Ramakrishnan, A.Ramsey, D.A.Rasmussen, M.H.Redi, G.Renda, G.Rewoldt, D.Roberts, J.Rogers, R.Rossmassler, A.L.Roquemore, E.Ruchov, S.A.Sabbagh, M.Sasao, G.Schilling, J.Schivell, G.L.Schmidt, R.Scillia, S.D.Scott, T.Senko, R.Sissingh, C.Skinner, J.Snipes, P.Snook, J.Stencel, J.Stevens, T.Stevenson, B.C.Stratton, W.Stodiek, E.Synakowski, W.Tang, G.Taylor, J.Terry, M.E.Thompson,

J.R.Timberlake, H.H.Towner, A.vonHalle, C.Vannoy, R.Wester, R.Wieland, J.B.Wilgen, M.Williams, J.R.Wilson, J.Winston, K.Wright, D.Wong, K.L.Wong, P.Woskov, G.A.Wurden, M.Yamada, A.Yeun, S.Yoshikawa, K.M.Young, M.C.Zarnstorff, and S.J.Zweben, Phys. Rev. Lett., **72**, (1994), 3526.

[26] R.J. Hawryluk, H. Adler, P. Alling, C.Ancher, H.Anderson, J.L.Anderson, J.W.Anderson, V.Arunasalam, G.Ascione, D.Ashcroft, C.W.Barnes, G.Barnes, S.Batha, M.G.Bell, R.Bell, M.Bitter, W.Blanchard, N.L.Bretz, C.Brunkhorst, R.Budny, T.Burgess, H.Bush, C.E.Bush, R.Camp, M.Caorlin, H.Carnevale, S.Cauffman, Z.Chang, C.Z.Cheng, J.Chrzanowski, J.Collins, G.Coward, M.Cropper, D.S.Darrow, R.Daugert, J.DeLooper, H.Duong, L.Dudek, R.Durst, P.C.Efthimion, D.Ernst, J.Faunce, R.Fisher, R.J.Fonck, E.Fredd, E.Fredrickson, N.Fromm, G.Y.Fu, H.P.Furth, V.Garzotto, C.Gentile, G.Gettelfinger, J.Gilbert, J.Gioia, T.Golian, N.Gorelenkov, B.Grek, L.R.Grisham, G.Hammett, G.R.Hanson, W.Heidbrink, H.W.Herrmann, K.W.Hill, H.Hsuan, A.Janos, D.L.Jassby, F.C.Jobes, D.W.Johnson, J.Kamperschroer, J.Kesner, H.Kugel, S.Kwon, G.Labik, N.T.Lam, P.H.LaMarche, E.Lawson, B.LeBlanc, M.Leonard, J.Levine, F.M.Levinton, D.Loesser, D.Long, M.J.Loughlin, J.Machuzak, D.K.Mansfield, M.Marchlik, E.S.Marmar, R.Marsala, A.Martin, G.Martin, V. Mastrocola, E.Mazzucato, R.Majeski, M.Mauel, M.P.McCarthy, B.McCormack, D.C.McCune, K.M.McGuire, D.M.Meade, S.S.Medley, D.R.Mikkelsen, S.L.Milora, D.Mueller, M.Murakami, J.A.Murphy, A.Nagy, G.A.Navratil, R.Nazikian, R.Newman, T.Nishitani, M.Norris, T.O'Conner, M.Oldaker, J.Ongena, M.Osakabe, D.K.Owens, H.Park, W.Park, S.F.Paul, Yu.I.Pavlov, G.Pearson, F.Perkins, E.Perry, R.Persing, M.Petrov, C.Kieras-Phillips, S.Pitcher, S.Popovichev, R.Pysher, A.L.Qualls, S.Raftopoulos, R.Ramakrishnan, A.Ramsey, D.A.Rasmussen, M.H.Redi, G.Renda, G.Rewoldt, D.Roberts, J.Rogers, R.Rossmassler, A.L.Roquemore, E.Ruchov, S.A.Sabbagh, M.Sasao, G.Schilling, J.Schivell, G.L.Schmidt, R.Scillia, S.D.Scott, T.Senko, R.Sissingh, C.Skinner, J.Snipes, P.Snook, J.Stencel, J.Stevens, T.Stevenson, B.C.Stratton, J.D.Strachan, W.Stodiek, E.Synakowski, W.Tang, G.Taylor, J.Terry, M.E.Thompson, J.R.Timberlake, H.H.Towner, A.vonHalle, C.Vannoy, R.Wester, R.Wieland, J.B.Wilgen, M.Williams, J.R.Wilson, J.Winston, K.Wright, D.Wong, K.L.Wong, P.Woskov, G.A.Wurden, M.Yamada, A.Yeun, S.Yoshikawa, K.M.Young, M.C.Zarnstorff, and S.J.Zweben, Phys. Rev. Lett., **72**, (1994), 3530

[27] JET Team, in Proceedings of the Fifteenth International Conferenceon Plasma

Physics and Controlled Nuclear Fusion Research, (Seville, Spain, September/October 1994), (International Atomic Energy Agency, Vienna, Austria) Vol. I, 211, Paper IAEA-CN-60/A2-4

[28] E. Lazarus, A.W. Hyatt, T.H. Osbornem S.E. Attenberger, M.E. Austin, K.H. Burrell, T.A. Kasper, M.S. Chu, J.W. Cuthbertson, E.J. Doyle, P. Gohil, J.M. Greene, C.M. Greenfield, R.J. Groebner, W.A. Houlberg, C.-L. Hsieh, G.L. Jackson, J. Kim, S. Konoshima, L.L. Lao, C. Lasnier, A.W. Moyer, C.L. Rettig, B. Rice, M.J. Schaffer, D.P. Schissel, R.T. Snider, R.D. Stambaugh, R.E. Stockdale, T.S. Taylor, A.D. Turnbull, M.R. Wade, R. Wood, and D. Wroblewski, in Proceedings of the Fifteenth International Conferenceon Plasma Physics and Controlled Nuclear Fusion Research, (Seville, Spain, September/October 1994), (International Atomic Energy Agency, Vienna, Austria) Vol. I, 31, Paper IAEA-CN-60/A1-2

[29] B.W. Rice, B.W Stallard, E.J. Strait, T.C. Luce, T.S. Taylor, C.M. Freenfield, F. Soldner, S. Sips, E.J. Lazarus, R. Maingi, M.R., Wade, Bull. of APS, 37th Annual meeting of the Division of Plasma Physics, paper 2F3, (1996) 1387

[30] C.M., Greenfield, J.C. DeBoo, T.H., Osborne, D. Boucher, F.W. Ferkins, M.N. Rosenbluth, and J. Wesley, Bull. of APS, 36th Annual meeting of the Division of Plasma Physics, paper 5P2, (1994) 1644

[31] B.W. Rice, K.H. Burrell, L.L. Lao, G. Navratil, B.W. Stallard, E.J. Strait, T.S. Taylor, M.E. Austin, T.A. Casper, M.S. Chu, C.B. Forest, P. Gohil, R.J. Groebner, W.W. Heidebrink, A.W. Hyatt, H. Ikezi, R.J. La Haye, E.A. Lazarus, Y.R. Lin-Liu, M.E. Mauel, W.H. Meyer, C.L. Rettig, DP. Schissel, H.E. St. John, P.L. Taylor, A.D. Turnbull, and the DIII-D Team, in Phys. of Plasma **3**, (1996), 1983.

[32] JT-60U Team, in Proceedings of the Fifteenth International Conference on Plasma Physics and Controlled Nuclear Fusion Research, (Seville, Spain, September/October 1994), (International Atomic Energy Agency, Vienna, Austria) Vol. I, 31, Paper IAEA-CN-60/A1-2

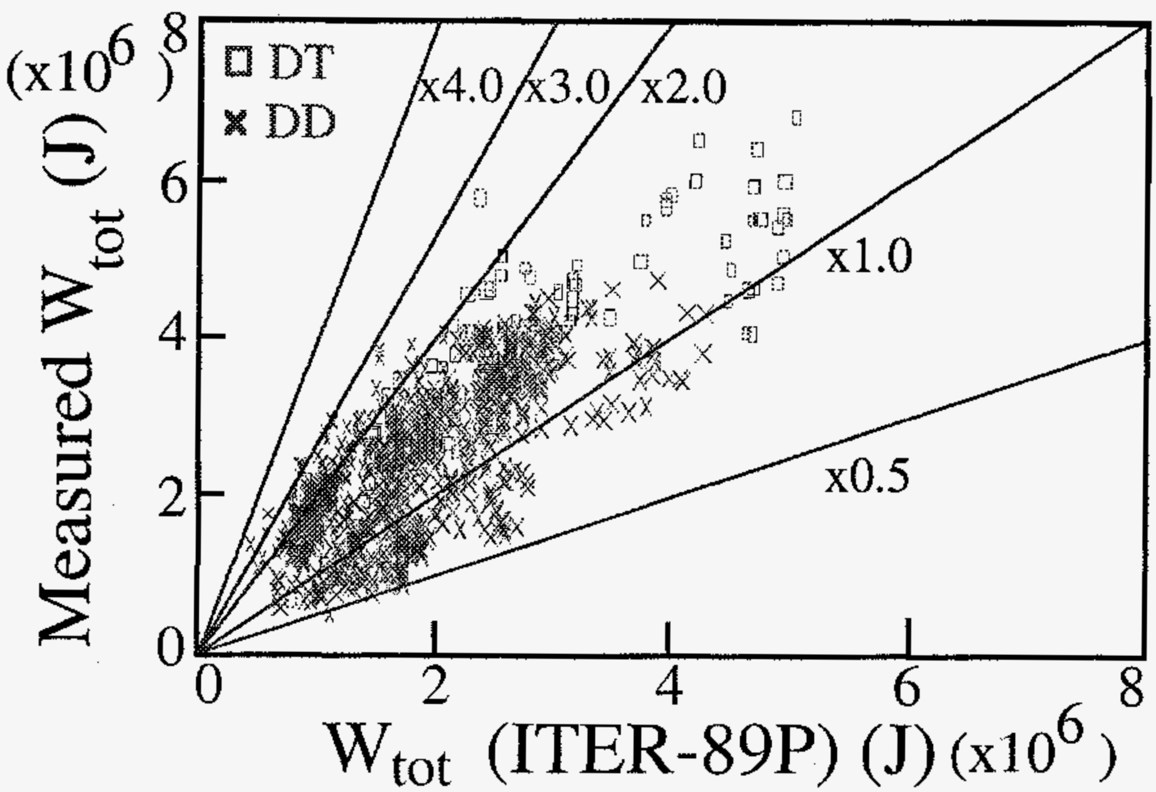

(x10⁶)
Measured $W_{tot}$ (J)
DT
DD
x4.0
x3.0
x2.0
x1.0
x0.5
0
2
4
6
8
$W_{tot}$ (ITER-89P) (J) (x10⁶)


Fig. 1 (a)

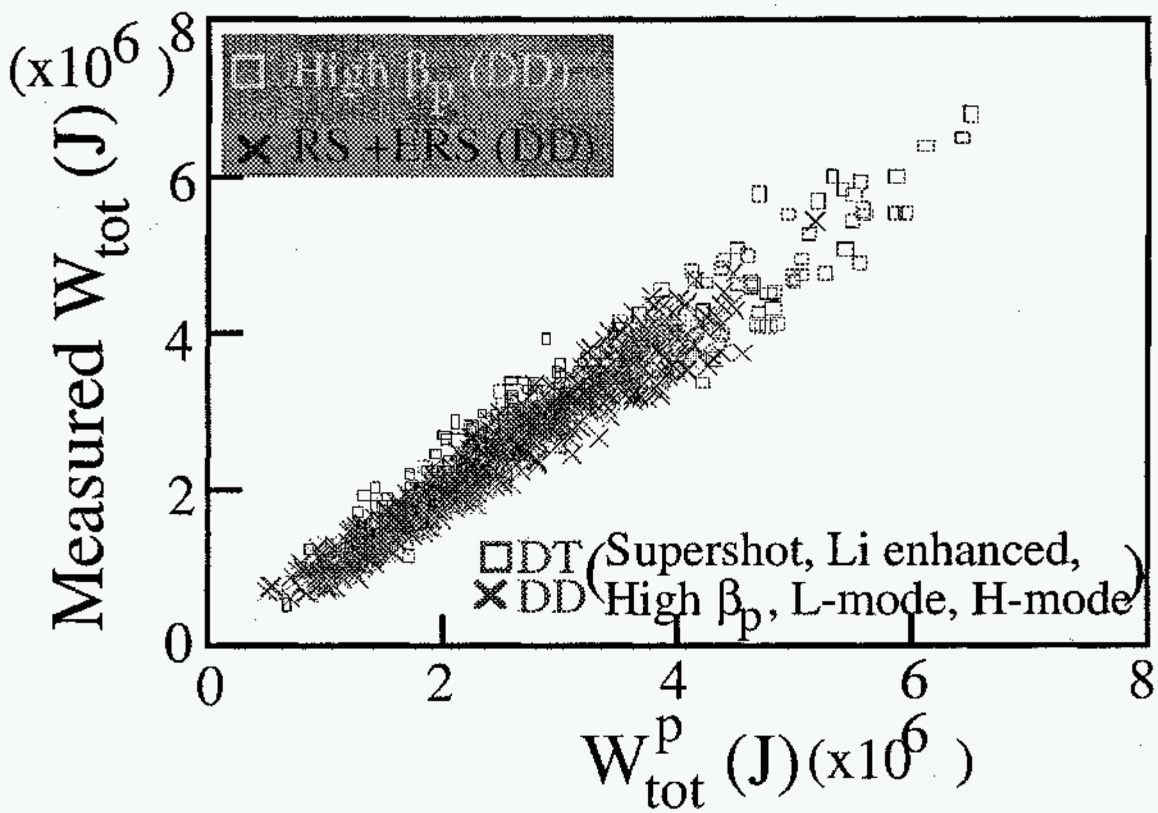

(x10^6 )
Measured W_tot (J)
High β_p (DD)
RS +ERS (DD)
DT
DD
(Supershot, Li enhanced, High β_p, L-mode, H-mode)
0
2
4
6
8
W^p_tot (J) (x10^6 )


Fig. 1 (b)

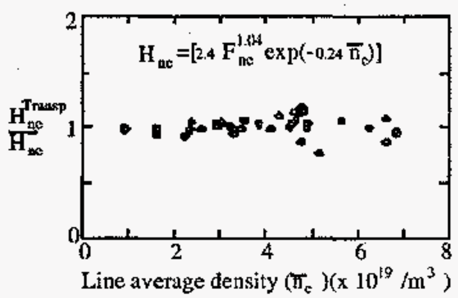
$H_{nc} = [2.4\ F_{nc}^{1.04} \exp(-0.24\ \overline{n}_e)]$
$\frac{H_{nc}^{Transp}}{H_{nc}}$
Line average density ($\overline{n}_e$ )(x $10^{19}$ /m$^3$ )

Fig. 2

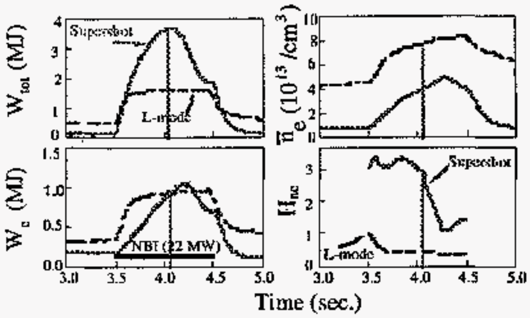
Supershot
L-mode
$W_{tot}$ (MJ)
$\overline{n}_e$ ($10^{13}$ /cm$^3$)
$W_e$ (MJ)
NBI (22 MW)
$H_{nc}$
Time (sec.)

Fig. 3

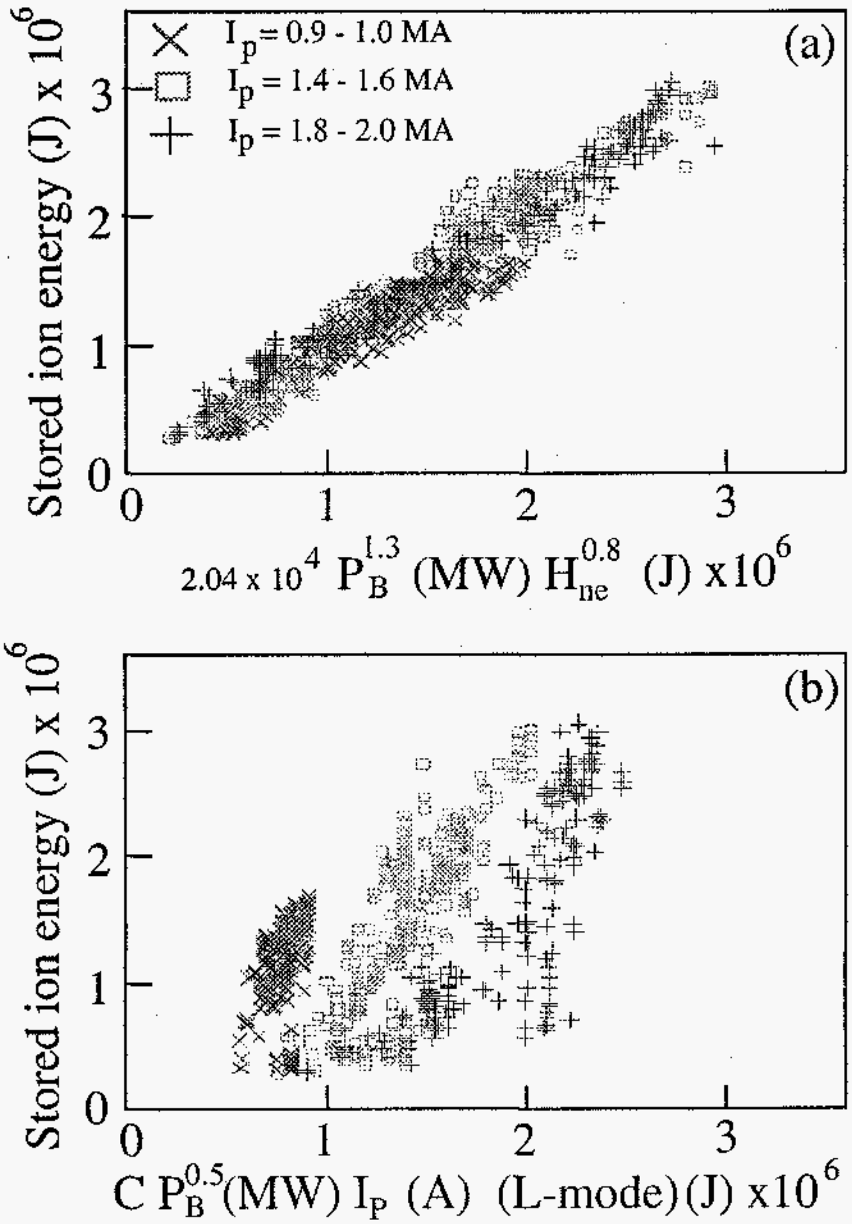

(a)
I p = 0.9 - 1.0 MA
Ip = 1.4 - 1.6 MA
Ip = 1.8 - 2.0 MA
Stored ion energy (J) x 10^6
2.04 x 10^4 P_B^1.3 (MW) H_ne^0.8 (J) x10^6
(b)
Stored ion energy (J) x 10^6
C P_B^0.5(MW) I_P (A) (L-mode)(J) x10^6


Fig. 4

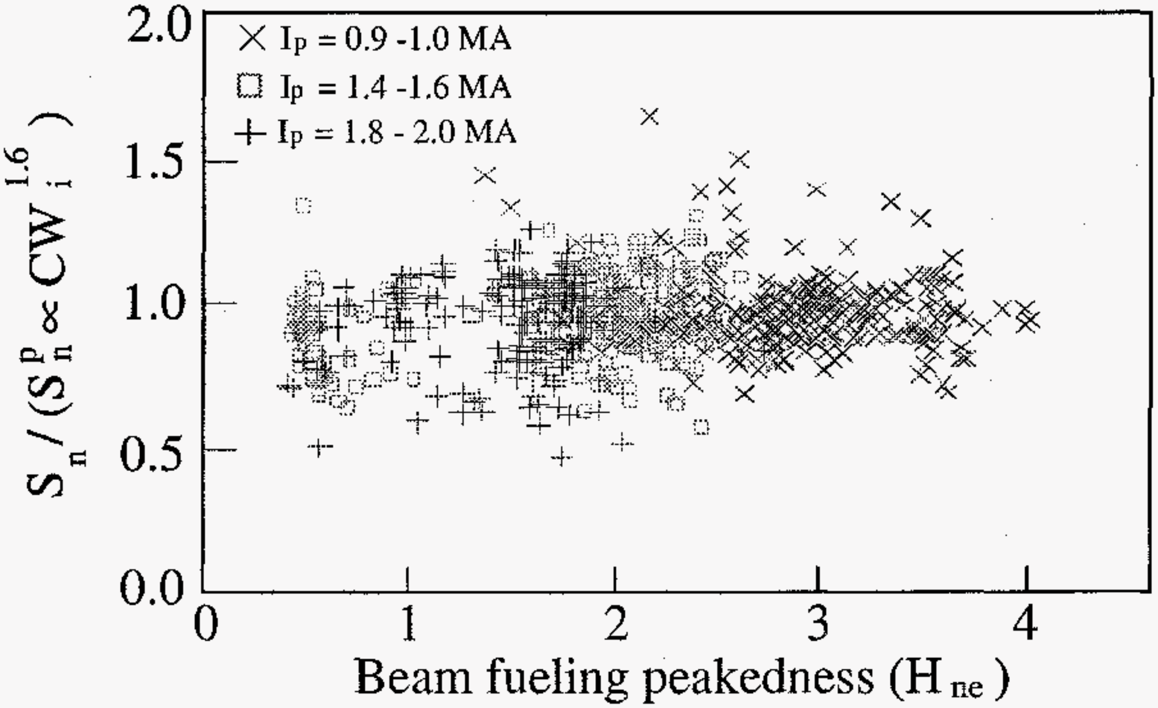

2.0
1.5
1.0
0.5
0.0
0
1
2
3
4
Ip = 0.9 -1.0 MA
Ip = 1.4 -1.6 MA
Ip = 1.8 - 2.0 MA
$S_n / (S_n^p \propto CW_i^{1.6})$
Beam fueling peakedness ($H_{ne}$)


Fig. 5

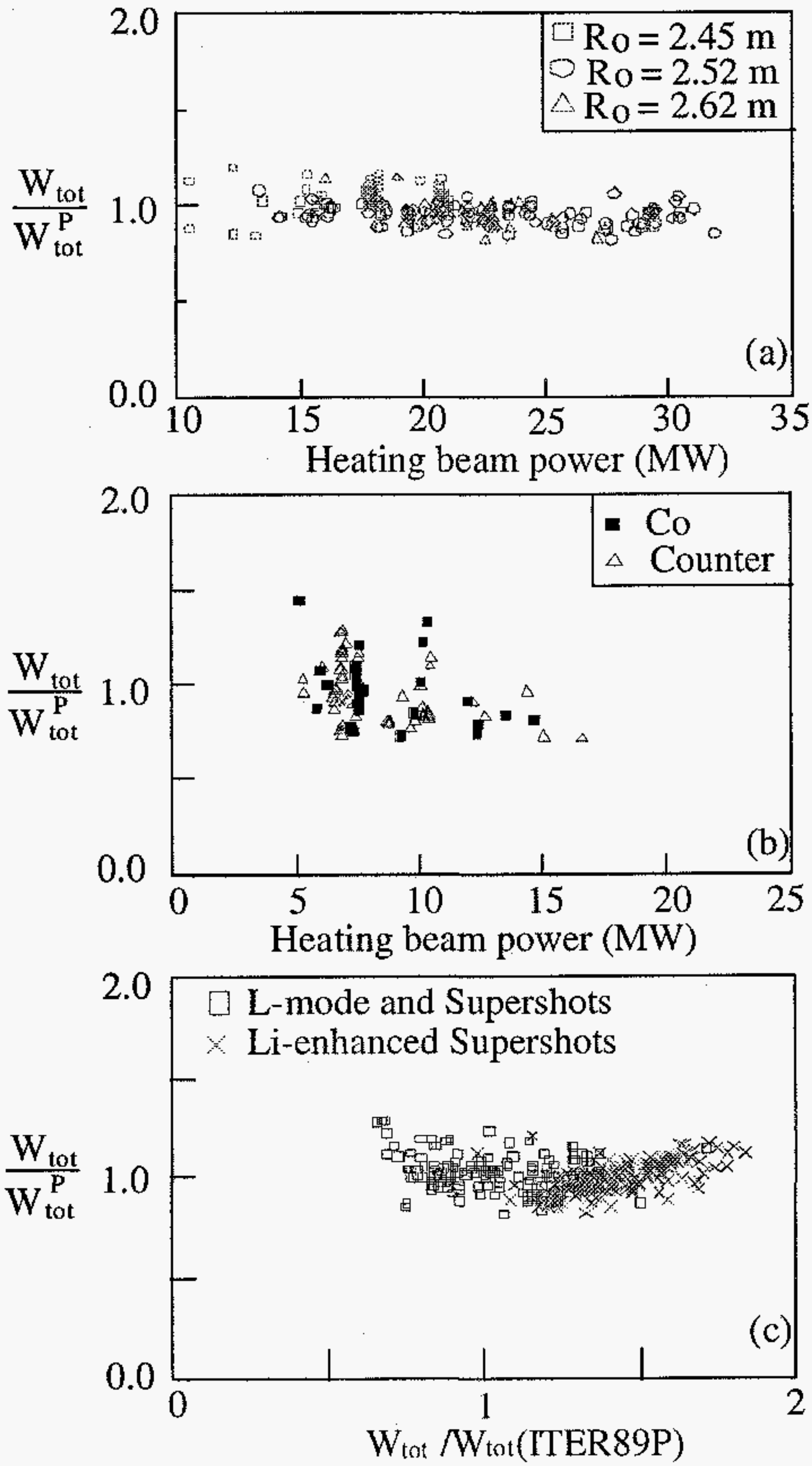

Ro = 2.45 m
Ro = 2.52 m
Ro = 2.62 m
(a)
Heating beam power (MW)
Co
Counter
(b)
Heating beam power (MW)
L-mode and Supershots
Li-enhanced Supershots
(c)
Wtot /Wtot(ITER89P)


Fig. 6

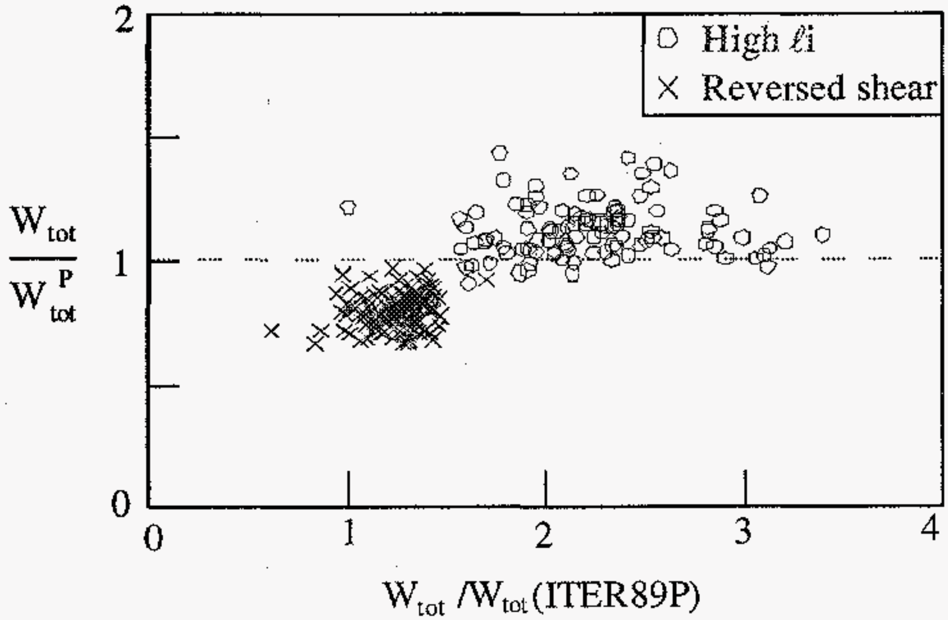

High ℓi
Reversed shear
2
1
0
0
1
2
3
4
$\frac{W_{tot}}{W_{tot}^{P}}$
$W_{tot}$ /$W_{tot}$(ITER89P)


Fig. 7

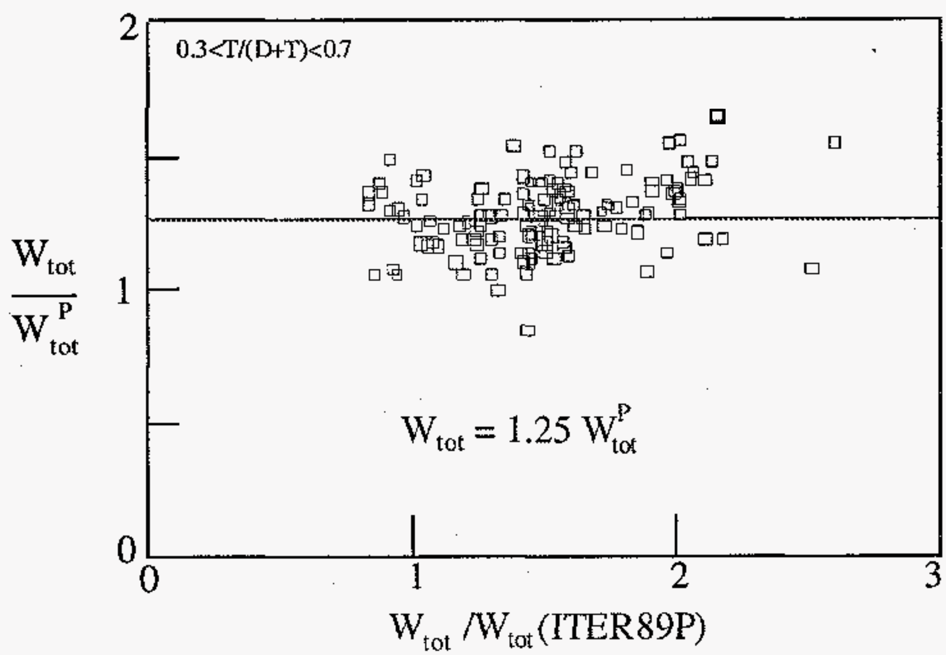

0.3<T/(D+T)<0.7
$W_{tot} = 1.25\ W_{tot}^{P}$
2
1
0
0
1
2
3
$\frac{W_{tot}}{W_{tot}^{P}}$
$W_{tot}$ /$W_{tot}$(ITER89P)


Fig. 8